J Med Sci 2023;43 (5):202-211 DOI: 10.4103/jmedsci.jmedsci 96 23

ORIGINAL ARTICLE



Elucidating the Role of SLC4A7 in Glioma Prognosis: A Comprehensive Approach Combining Bioinformatics, Single-Cell Analysis, and Tissue Validation

Tung Liu¹, Nien-Tzu Liu¹, Yu-Chuan Huang^{2,3}, Wei-Wen Hsu⁴, Yu-Chieh Lin^{5,6}, Yao-Feng Li^{1,6,7}

¹Department of Pathology, Tri-Service General Hospital, National Defense Medical Center, ²School of Pharmacy and Institute Pharmacy, National Defense Medical Center, ³Department of Research and Development, National Defense Medical Center, Taipei, ⁴Department of Computer Science and Information Engineering, National Taitung University, Taitung, ⁵Department of Pathology and Laboratory Medicine, Taoyuan Armed Forces General Hospital, Taoyuan, ⁶Graduate Institute of Medical Sciences, National Defense Medical Center, ⁷Graduate Institute of Life Sciences, National Defense Medical Center, Taipei, Taiwan

Background: Gliomas, prevalent and lethal brain tumors, present limited treatment options despite advancements in understanding their molecular features. SLC4A7, an SLC4 family member and potential biomarker, is involved in acid-base regulation, affecting cancer cell growth. Targeting this mechanism may offer new therapeutic strategies. Aim: This study examines SLC4A7's role in gliomas and its potential as a therapeutic target. Methods: Genomic, whole exon sequencing, and single-cell sequencing datasets from glioma patients were processed and analyzed, followed by gene set enrichment analysis (GSEA). Cellular components and immune cell populations were investigated using 12-cell state and CIBERSORT analyses. Tissue microarray and immunohistochemistry were employed, with an automated semi-quantitative system scoring staining. ANOVA determined the significance of immunostaining scores related to clinical parameters. Results: Our data found increased SLC4A7 in tumor components correlated with higher tumor grading and poorer prognosis. Immunohistochemistry confirmed a relationship between SLC4A7 protein expression with tumor grade and the proliferation index. GSEA linked high SLC4A7 to cell proliferation and inflammation signaling. PIK3CAs were identified as a potential upstream in IDH mutant glioma but not in IDH wildtype. A positive correlation between heightened SLC4A7 expression and tumor mutation burden suggested genomic instability's role in SLC4A7 upregulation. Cellular heterogeneity analysis highlighted the importance of inflammatory cells, particularly macrophage M0. Conclusion: This study emphasizes SLC4A7's significance in adult gliomas, associating increased expression with high tumor grade, poor prognosis, enhanced proliferation, and inflammation. Investigating SLC4A7 may provide insights into cancer biology and contribute to developing innovative therapeutic targets for improved brain tumor treatments.

Key words: SLC4A7, glioblastoma, the cancer genome atlas, Chinese glioma genome atlas, gene set enrichment analysis, tumor mutation burden, microsatellite instability, CIBERSORT, single-cell sequencing

INTRODUCTION

Brain tumors represent a significant cancer burden, with diffuse gliomas being the primary malignancy and glioblastomas the most lethal subtype. Recent research highlights the importance of molecular markers, such as IDH1/2, 1p19q, CDKN2A/B, EGFR amplification, 5

Received: April 11, 2023; Revised: May 02, 2023; Accepted: May 04, 2023; Published: July 16, 2023
Corresponding Author: Dr. Yao-Feng Li, Department of Pathology, Tri-Service General Hospital, National Defense Medical Center, No. 325, Sec. 2, Chenggong Rd., Neihu Dist., Taipei 114, Taiwan. Tel: +886-2-87923311 #13958; Fax: 02-6600-0309. E-mail: liyaofeng1109@gmail.com

chromosomal 7/10 alterations,⁵ TERT promoter mutation,⁵ and MGMT promoter methylation status,⁶ in determining prognosis and guiding treatment. The updated 5th edition of the WHO Classification of Tumors of the Central Nervous System incorporates these findings.³ Despite advancements

This is an open access journal, and articles are distributed under the terms of the Creative Commons Attribution-NonCommercial-ShareAlike 4.0 License, which allows others to remix, tweak, and build upon the work non-commercially, as long as appropriate credit is given and the new creations are licensed under the identical terms.

For reprints contact: WKHLRPMedknow_reprints@wolterskluwer.com

How to cite this article: Liu T, Liu NT, Huang YC, Hsu WW, Lin YC, Li YF. Elucidating the role of SLC4A7 in glioma prognosis: A comprehensive approach combining bioinformatics, single-cell analysis, and tissue validation. J Med Sci 2023;43:202-11.

in diagnosis, limited therapeutic options persist, with the standard of care involving gross total resection, chemotherapy, and radiotherapy, yielding a median survival of 14.6 months.⁷ Gliomas often resist first-line chemotherapy, temozolomide, prompting exploration of alternative therapeutic targets.

SLC4A7 is a member of the SLC4 family, which includes 10 genes,8 with at least 8 involved in HCO₃ transport across the plasma membrane. SLC4A1-3 function as cellular acid loaders, while SLC4A4, SLC4A5, SLC4A7, SLC4A8, and SLC4A10 typically act as acid extruders in normal cells, except for SLC4A4 in kidneys and SLC4A5 in the choroid plexus.^{8,9} Disruption of several SLC4 family members has been linked to cancer progression, such as breast cancer.¹⁰ Targeting glycolytic activity through phosphofructokinase-1 inhibition is a potential therapeutic strategy, as it is pH-sensitive and modulating acid-base regulation can selectively inhibit glycolysis in cancer cells without harming healthy tissue.8 Approaches include targeting Na⁺/H ⁺ exchangers, monocarboxylate transporters, H + pumps, NaHCO3 supplementation, or carbonic anhydrase inhibition.11 Recently, SLC4A4 (NBCe1) was found to play a crucial role in glioblastoma extracellular acidosis regulation.¹¹ Intriguingly, our biomarker screening identified SLC4A7 as a potential biomarker whose role in glioma remains unexplored. This study aims to elucidate SLC4A7's role in glioma through advanced bioinformatics, single-cell analysis techniques, and clinical validation using immunohistochemistry.

MATERIALS AND METHODS

Data collection for bioinformatics analyses

The analyzed datasets comprised three components: Genomic data, whole exon sequencing (WES), and single-cell sequencing data. The genomic data, including transcriptome expression, clinical parameters, and whole-exome sequencing data, were obtained from the cancer genome atlas (TCGA) and Chinese Glioma Genome Atlas (CGGA). A total of 703 cases from TCGA and 1018 cases from CGGA were reclassified into three subgroups based on the 2021 WHO classification: IDH wildtype astrocytoma, IDH mutant astrocytoma, and oligodendroglioma. In addition, 897 cases of WES data were collected to calculate tumor mutation burden (TMB) for further investigation. Finally, two single-cell sequencing datasets were downloaded from the gene-expression omnibus database (GEO), including IDH wildtype data (GSE131928) and IDH mutant data (GSE89567).

Data processing

R (version 4.1.0) and relevant packages were used for bioinformatics analyses. Gene expression data, RPKM (Reads Per Kilobase per Million), was converted to TPM (Transcripts Per Million). Limma and ggpubr packages were employed for mRNA quantification, regression, and differentially expressed gene analysis (adjusted P < 0.05). Kaplan-Meier and

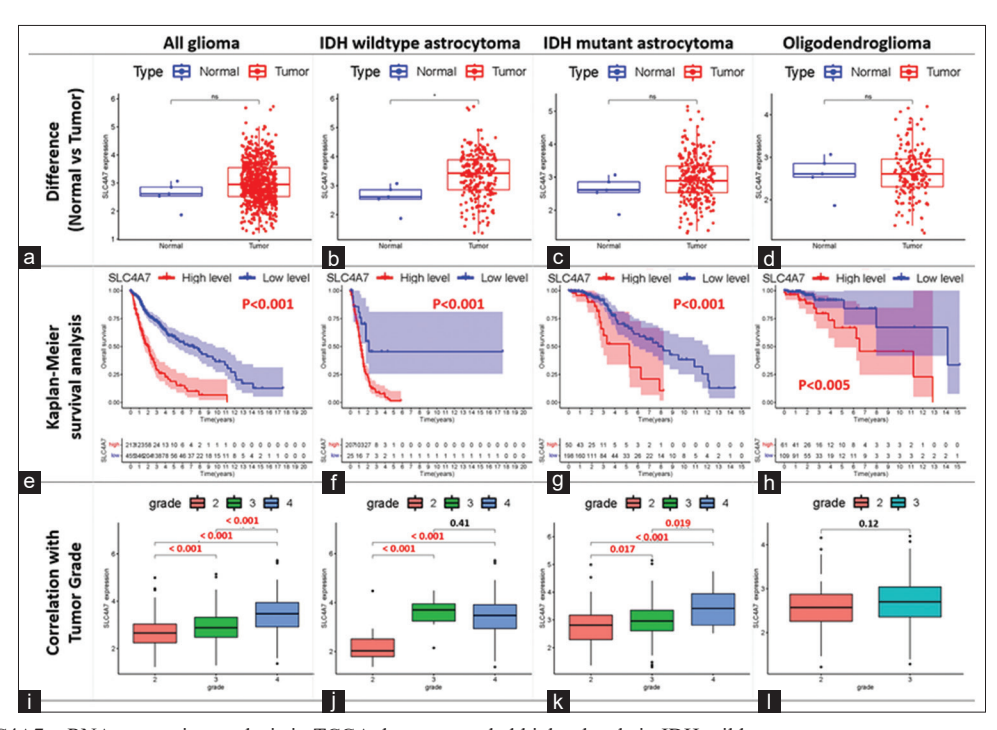


Figure 1: (a-d) SLC4A7 mRNA expression analysis in TCGA dataset revealed higher levels in IDH-wildtype astrocytoma tumor components, (e-h) poorer prognosis across all subgroups, (i-l) and positive correlation with tumor grading, except in oligodendroglioma. TCGA = The cancer genome atlas

COX-survival analyses assessed SLC4A7's impact on prognosis. TMB was calculated using WES data and the "maftools" package, while microsatellite instability (MSI) data from the landmark paper by the team of Sameek Roychowdhury¹² was used for analysis. Single-cell sequencing datasets GSE131928 and GSE89567 were analyzed on the BBrowser platform.¹³

Gene set enrichment analysis, 12-cell state, and CIBERSORT

Gene set enrichment analysis (GSEA) compared high and low-SLC4A7 expression groups in TCGA glioma datasets, using the "hallmark gene-sets v7.5" as a reference and default parameters. Then, we used bulk transcriptome data from TCGA and CGGA databases to determine the proportions of 12-cell components using 12-cell state prediction¹⁴ and 22 immune cells for each case by CIBERSORT¹⁵ to investigate correlations with SLC4A7 expression.

Tissue microarray and immunohistochemistry

Glioma tissue microarray (TMA) (GL1001a) was obtained from Biomax, Inc. This TMA included 73 cases of glioma (7 for Gr 1; 46 for Gr 2; 11 for Gr 3; 9 for Gr 4) and 9 normal

brain tissue. We employed the Ventana Benchmark®XT immunostainer to perform consistent immunohistochemical staining. Antigen retrieval was performed, and primary antibodies included SLC4A7 (Abcam #ab82335), Ki67 (Abcam #ab15580), and P53 (Cell Signaling #2524). Positive and negative controls were used.

Immunohistochemistry scoring

Consistent with prior publications,^{16,17} stained slides were evaluated and scored employing an automated semi-quantitative system using Image J Fiji software. The quantified staining intensity ranged from 0 to 3. A percentage of tumor cells stained from 0% to 100% was estimated, resulting in an Immunoscore from 0 to 300 based on the sum of each staining intensity multiply its corresponding staining percentage.

Statistical analysis

ANOVA assessed the significance of immunostaining scores concerning clinical parameters using SPSS Statistics Version 22.0 (Armonk, NY: IBM Corp, American).

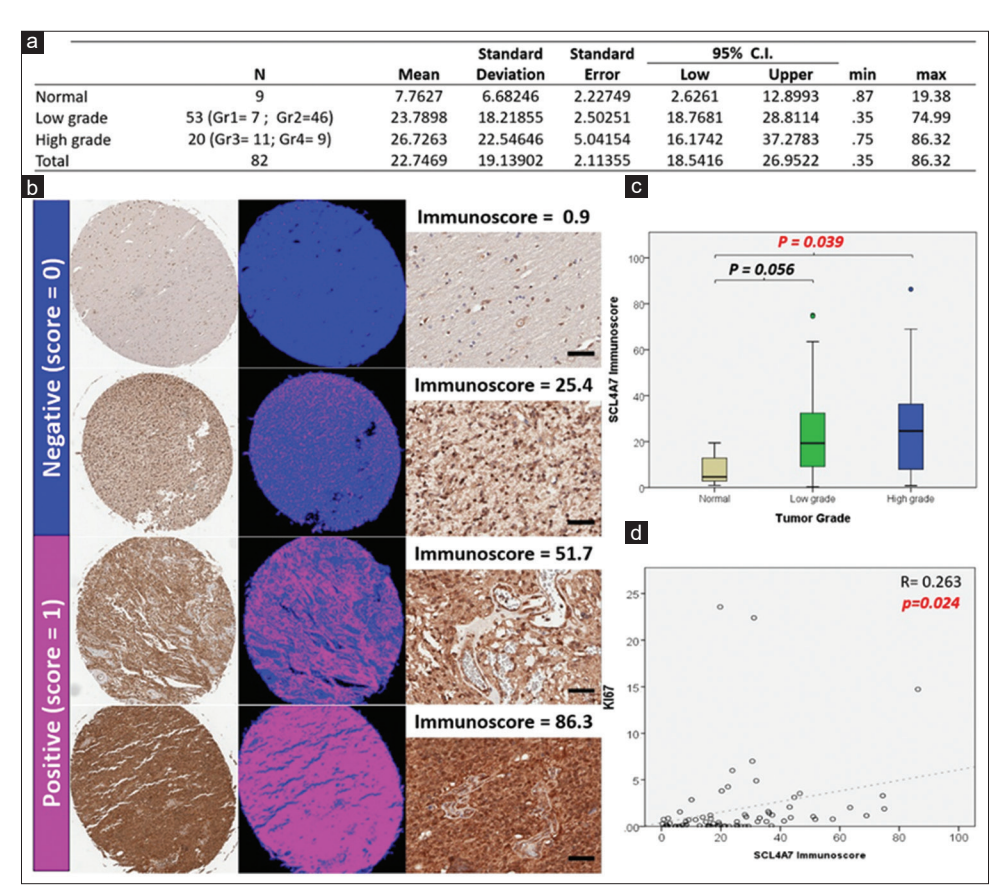


Figure 2: (a and b) SLC4A7 protein expression was validated using immunohistochemistry in 82 clinical cases, (c) correlated with tumor grading, and (d) the Ki67 labeling index

RESULTS

Result 1: SLC4A7 increased in tumor and correlates with tumor grading and poorer prognosis.

Our bioinformatics analysis revealed significantly increased SLC4A7 expression in tumor components versus normal tissue in IDH-wildtype astrocytoma [Figure 1a and b], but not in IDH-mutant astrocytoma or oligodendroglioma [Figure 1c and d]. Kaplan-Meier survival analysis demonstrated a significant association between higher SLC4A7 levels and worse prognosis across subgroups [Figure 1e-h]. Additionally, SLC4A7 correlated positively with tumor grade in pan-glioma, IDH-wildtype, and IDH-mutant astrocytoma [Figure 1i-k], but not in oligodendroglioma [Figure 11].

Result 2: SLC4A7 protein expression correlated with tumor grade and proliferation.

To verify SLC4A7 protein expression at the tissue level, we conducted immunohistochemistry on 82 clinical cases [Figure 2a] and processed images using Image J software. Staining intensity was scored (0 for negative, 1 for positive) alongside the percentage staining area (0%–100%). The Immunocore was calculated as the intensity multiplied by the staining area percentage. Results are displayed in [Figure 2b] and Supplementary. Statistical analysis showed SLC4A7 expression correlating with tumor grading [Figure 2c],

consistent with transcriptome data. A significant association between elevated SLC4A7 expression and Ki67 labeling index was also observed [r = 0.263, P = 0.024, Figure 2d].

Result 3: The higher SLC4A7 expression is associated with cell proliferation signaling and inflammation.

GSEA analyses were employed to investigate altered signaling pathways linked to increased SLC4A7 expression in subgroups using TCGA datasets. The top 5 altered gene sets of each group showed [Figure 3a-c] included three intersecting sets (E2F_TARGETS, G2M_CHECKPOINT, MITOTIC_SPINDLE) related to cell proliferation [Figure 2d], aligning with the previous discovery, that higher SLC4A7 correlated with Ki67. Additionally, recurrent gene sets among astrocytoma subgroups, including INFLAMMATORY_RESPONSE, INTERFERON_GAMMA_RESPONSE, and TNFA_SIGNALING_VIA_NFKB, indicated heightened inflammation [Figure 3d and e].

Result 4: PIK3CA might be a potential driver of SLC4A7 upregulation in IDH mutant glioma but not in the IDH wildtype.

We analyzed transcriptomic data and WES results to identify potential driver genes for SLC4A7 upregulation. Then, we obtained lists of associated genes for each group by assessing SLC4A7 expression correlation with mutation status across 14,733 genes. Our data found no shared gene among

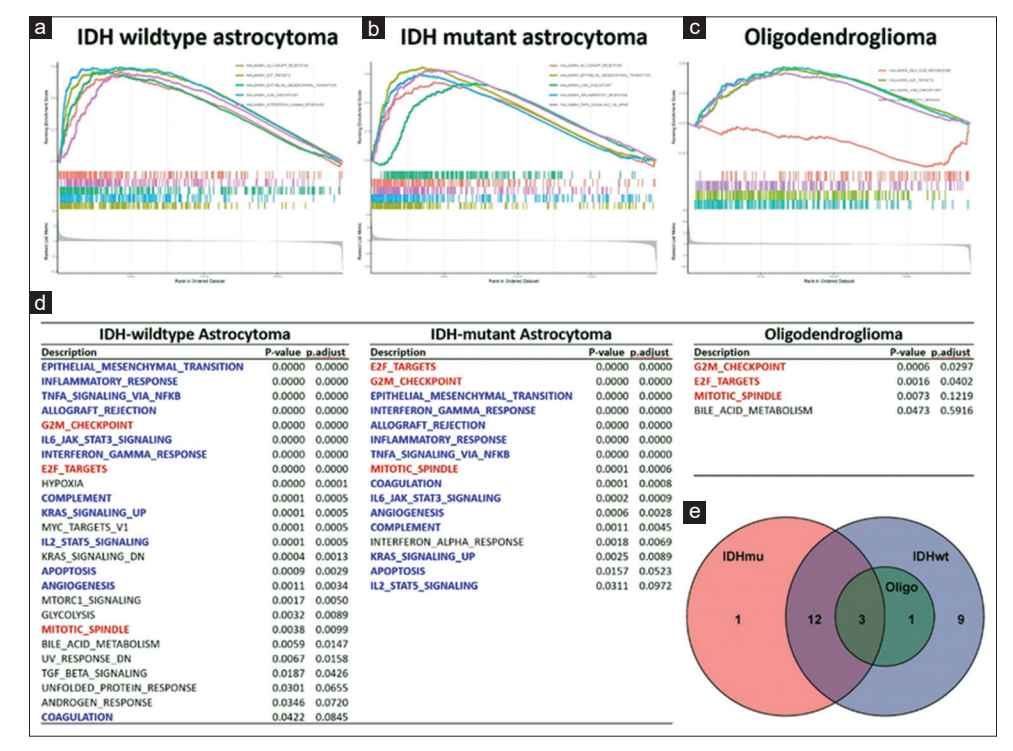


Figure 3: (a-c) Top 5 altered gene sets in each subgroup from GSEA. (d-e) There were three intersecting sets, including E2F_TARGETS, G2M_CHECKPOINT, and MITOTIC_SPINDLE, associated with proliferation signalling. Additionally, increased inflammation is also noted in both astrocytoma subgroups. GSEA=Gene set enrichment analysis

all three subgroups [Figure 4]. However, PIK3CA emerged in IDH mutant astrocytoma and oligodendroglioma but was absent in IDH wildtype [Figure 4].

Result 5: SLC4A7 positive correlates to TMB but reversely to MSI.

Besides a single gene affecting SLC4A7 expression, genomic stability might also play a role. Hence, we investigate TMB and MSI indicators, finding a positive correlation between SLC4A7 and TMB in all adult glioma subgroups [Figure 5a-c]. However, an inverse relationship was found between SLC4A7 expression and MSI only in the IDH wildtype group [Figure 5d], with no significant association in the other groups [Figure 5e and f].

Result 6: Besides tumors, inflammatory cells played roles in the expression of SLC4A7.

To assess the effects of tumor diversity on SLC4A7 expression, we examined single-cell sequencing data from both IDH wildtype and mutant astrocytomas. Upon inspecting the SLC4A7 expression heatmap, we observed that its expression was primarily associated with myeloid and T cell

lineages and a minor subset of tumor cells in IDH wildtype astrocytoma [Figure 6a and b]. A significant difference was found between tumor and reactive glia [P < 0.001, Figure 6c]. Furthermore, the comparisons between myeloid and tumor cells, T cells, and reactive glia all displayed statistical significance [P < 0.001, Figure 6f]. A similar pattern emerged in the IDH mutant astrocytoma dataset, as SLC4A7 expression was also correlated with myeloid cells, T cells, and a portion of tumor cells [Figure 6d and e]. The distinction between tumor and reactive glial cells exhibited statistical significance [P < 0.001, Figure 6f]. Additionally, comparisons of myeloid cells to tumor cells and reactive glial cells yielded statistically significant differences [P < 0.001, Figure 6f].

Result 7: SLC4 correlation with tumor components varies by IDH status.

We deconvoluted bulk transcriptomes into 12 cellular states ¹⁴ and 22 immune cells ¹⁵ to study SLC4A7 correlation. In TCGA and CGGA databases, SLC4A7 correlations varied with IDH status [Table 1]. IDH wildtype positively correlated with differentiated tumor components negative with stem cells; IDH

	IDH	wt		IDH	mu	Ol	igo
Gene	p_value	Gene	p_value	Gene	p_value	Gene	p_value
FBN2	0.0021	AKAP9	0.03	РІКЗСА	0.0014	HDAC2	0.007
FER1L6	0.0063	DUSP27	0.03	ACACA	0.0045	DCHS1	0.011
CSMD3	0.0069	FAM71B	0.03	SPATA31D1	0.0091	USP11	0.016
MAP3K19	0.0076	GABRD	0.03	UGT2B4	0.0093	BCOR	0.024
SERINC2	0.0082	MYO9B	0.03	EXPH5	0.011	PIK3CA	0.025
ATCAY	0.011	OR51T1	0.03	IL16	0.014	EPC2	0.029
PGR	0.012	MYH2	0.031	PPP2R2D	0.015	NOTCH1	0.042
PHF3	0.012	SFI1	0.031	TP53	0.015	ALMS1	0.043
SORT1	0.013	ANK1	0.032	NPAP1	0.017		
PCDHGA5	0.015	NRIP1	0.032	RASEF	0.02		
FLT1	0.016	NTN4	0.032	NLRP8	0.031		
G6PC	0.016	PCDHGA7	0.032	KMT2D	0.035		
SEL1L2	0.016	ATP11C	0.036	F13B	0.042		
DNAH3	0.017	ABCC10	0.037	PKHD1	0.042		
KL	0.017	ATF7IP	0.037	RYR2	0.046		
NCKAP1L	0.017	OR5A1	0.037				
SLC28A1	0.017	PRX	0.037				
CLCA1	0.02	AGBL5	0.038	/ 15		011	
COL4A5	0.02	NCKAP5	0.038	/ IL	Hmu	Oligo	\
GABRA6	0.02	CPD	0.039	1			1
MCTP2	0.02	TENM4	0.04		14	(1) 7	
PCDHGA2	0.02	DLC1	0.041	\			/
RTTN	0.02	IGHG4	0.041			X	
LAMA5	0.021	NF1	0.041		,		
RPL10L	0.021	WDR78	0.042		_//		
ATR	0.022	KIAA2026	0.043				
LTBP1	0.022	ANK3	0.044				
SCN10A	0.022	OR52M1	0.044				
SP110	0.022	CALN1	0.045			70	
GALNT5	0.023	OR51A4	0.045				
МҮО7В	0.024	AHNAK2	0.047				
SH3TC2	0.026	COBLL1	0.047				
MXRA5	0.027	CTIF	0.047			IDHwt /	
PCDHA7	0.028	ABLIM3	0.048			Diwi	
LRRC30	0.029	GRIA1	0.049				

Figure 4: PIK3CA mutation correlated with SLC4A7 expression in IDH mutant astrocytoma and oligodendroglioma, but not IDH wildtype

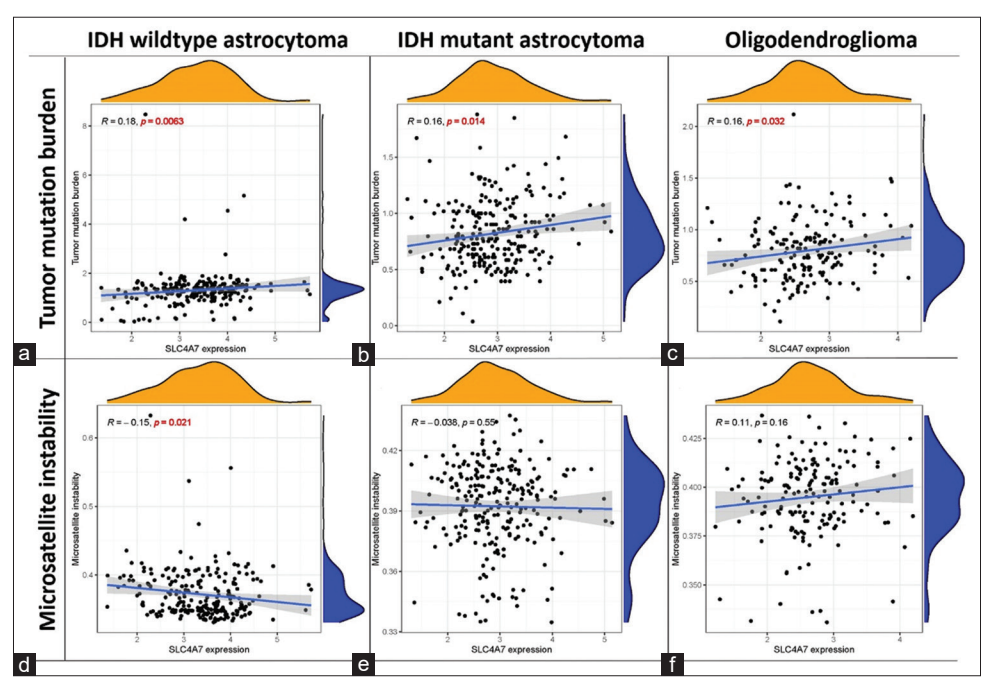


Figure 5: SLC4A7 expression and genomic stability association. (a-c) SLC4A7 correlated with TMB in all glioma subgroups (d-f) Inversely with MSI in IDH wildtype only. TMB = Tumor mutation burden, MSI = Microsatellite instability

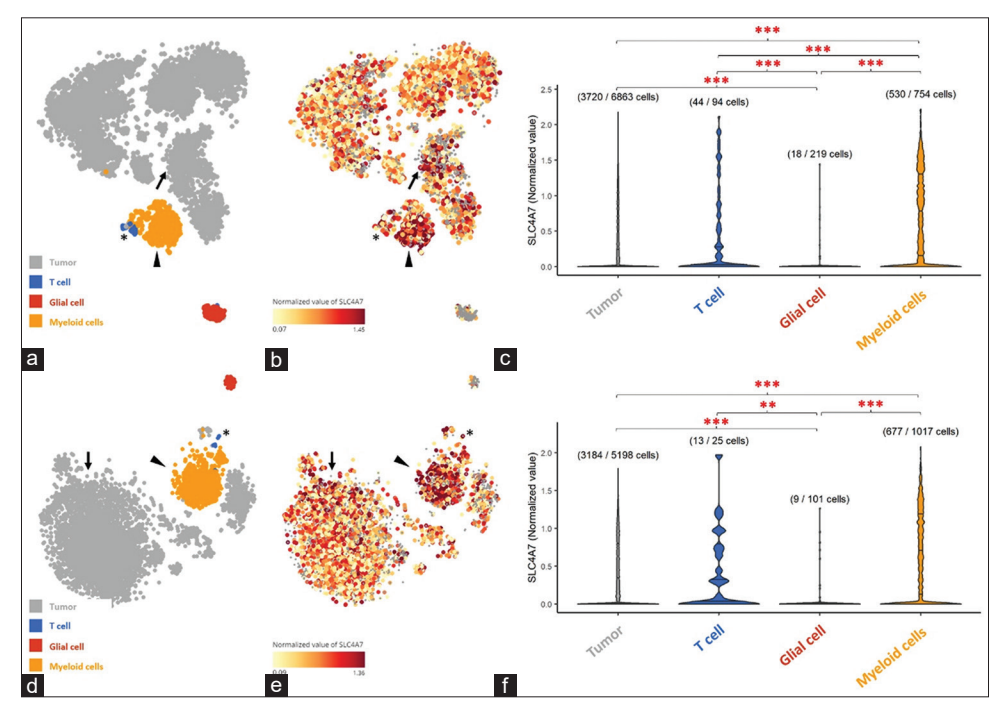


Figure 6: (a and b) SLC4A7 heatmap shows a strong association with myeloid (arrow head) and T cells (asterisk) and a minor subset of tumor cells (arrow) in IDH wildtype astrocytoma. (c) Significant differences in tumor vs. reactive glia, and myeloid vs. tumor cells, T cells, and reactive glia. (d-f) A similar pattern in IDH mutant astrocytoma, with significant differences between tumor to reactive glia and myeloid cells to tumor cells/reactive glia, emphasizes tumor heterogeneity's impact on SLC4A7 expression

mutant correlated with proliferative tumor cells. Most stromal cells showed decreased expression with increased SLC4A7, except fibroblasts. Immune composition showed increased

myeloid and granulocyte populations and decreased dendritic cells with elevated SLC4A7 [Table 1]. Using CIBERSORT, SLC4A7 was significantly associated with increased M0

Table 1: SLC4A7 correlation with tumor components varies by isocitrate dehydrogenase status

	,	IDi	Hwt	IDI	Hmu	Oligo		
		TCGA	CGGA	TCGA	CGGA	TCGA	CGGA	
		n=233	n=447	n=247	n=352	n=182	n=214	
Stemcell_tumor	correlation	-0.147*	-0.104*	-0.027	0.147**	0.107	0.148*	
	P	0.025	0.028	0.674	0.006	0.151	0.031	
Prolif_stemcell_tumor	correlation	0.073	0.052	0.318**	0.200**	0.405**	0.040	
	P	0.269	0.273	0.000	0.000	0.000	0.556	
Differentiated_tumor	correlation	0.066	0.115*	-0.110	-0.140**	-0.057	-0.002	
	P	0.316	0.015	0.084	0.009	0.441	0.978	
Oligodendrocyte	correlation	-0.331**	-0.246**	-0.228**	-0.122*	-0.278**	-0.194**	
	P	0.000	0.000	0.000	0.022	0.000	0.004	
Pericyte	correlation	-0.055	-0.001	-0.196**	-0.139**	-0.256**	-0.041	
	P	0.400	0.984	0.002	0.009	0.000	0.549	
Endothelial	correlation	-0.159*	-0.247**	-0.160*	-0.376**	-0.200**	-0.352**	
	P	0.015	0.000	0.012	0.000	0.007	0.000	
Fibroblast	correlation	0.220**	0.060	0.153*	-0.047	0.155*	-0.197**	
	P	0.001	0.206	0.016	0.384	0.036	0.004	
Myeloid	correlation	0.168*	0.159**	0.333**	-0.016	0.153*	-0.247**	
	P	0.010	0.001	0.000	0.770	0.039	0.000	
Granulocyte	correlation	0.275**	0.179**	0.452**	0.098	0.335**	0.040	
	P	0.000	0.000	0.000	0.065	0.000	0.557	
Dendritic_cell	correlation	-0.150*	-0.100*	-0.151*	-0.098	-0.159*	0.066	
	P	0.022	0.035	0.017	0.067	0.032	0.333	
T_cell	correlation	0.008	-0.163**	-0.050	-0.146**	-0.083	-0.142*	
	P	0.903	0.001	0.436	0.006	0.268	0.038	
B_cell	correlation	-0.075	0.013	.c	.a	.c	0.062	
	P	0.252	0.787				0.363	

TCGA: The Cancer Genome Atlas, CGGA: Chinese Glioma Genome Atlas, IDHwt: Isocitrate dehydrogenase wildtype, IDHmu: Isocitrate dehydrogenase mutant, SLC4A7: Solute Carrier Family 4 Member 7

macrophage, depleted monocytes [Table 2], higher granulocyte functions (eosinophils, neutrophils), and decreased T and NK populations.

DISCUSSION

Although brain tumor diagnosis has significantly improved, treatment options remain limited, necessitating the identification of potential therapeutic targets. This study focused on SLC4A7, a gene encoding Sodium Bicarbonate Cotransporter 3 (NBCn1), which regulates intracellular pH and bicarbonate transport, essential for cellular processes such as migration, invasion, and proliferation. Genetic variations in SLC4A7, such as single nucleotide polymorphisms, have been linked to increased breast cancer risk. ¹⁰ These variations may affect the encoded protein's function, leading to dysregulated

intracellular pH and bicarbonate transport, contributing to cancer development and progression. Recently, SLC4A4 (NBCe1) has also been identified to play a critical role in regulating extracellular acidosis in glioblastoma. Our biomarker screening identified SLC4A7 as a potential biomarker with an unclear role in glioma.

To better understand SLC4A7's connection to tumor proliferation and inflammation, we employed single-cell sequencing, 12-cell state prediction, and CIBERSORT to examine tumor and immune heterogeneity impacts. SLC4A7 expression was associated with myeloid lineage and a small subset of tumor cells, correlating with increased myeloid cells. CIBERSORT analyses revealed increased inflammation primarily related to higher M0 macrophage numbers in IDH wildtype astrocytoma and oligodendroglioma groups, while monocyte depletion suggested conversion to macrophages.

Table 2: SLC4A7 correlation with immune composition, particularly M0 macrophage activation, and monocyte depletion

		ID	Hwt	IDI	Hmu	Oligo		
		TCGA	CGGA	TCGA	CGGA	TCGA	CGGA	
		n=49	<i>n</i> =112	n=86	n=136	n=14	n=24	
B_cells_naive	correlation	-0.028	0.240*	-0.083	0.032	-0.256	.a	
	P	0.851	0.011	0.450	0.707	0.376		
B_cells_memory	correlation	0.001	-0.317**	0.007	-0.139	-0.067	-0.225	
	P	0.995	0.001	0.951	0.108	0.819	0.291	
Plasma_cells	correlation	-0.161	-0.127	-0.087	-0.130	0.048	-0.181	
	P	0.269	0.182	0.424	0.132	0.871	0.397	
T_cells_CD8	correlation	0.042	-0.089	-0.103	0.012	-0.214	-0.225	
	P	0.772	0.352	0.345	0.893	0.462	0.291	
T_cells_CD4_naive	correlation	.a	-0.243**	-0.056	-0.172*	.a	0.172	
	P		0.010	0.607	0.045		0.422	
T_cells_CD4_memory_resting	correlation	-0.032	0.132	0.027	0.102	0.434	0.081	
	P	0.828	0.165	0.805	0.237	0.121	0.708	
T_cells_CD4_memory_activated	correlation	-0.070	0.173	0.269*	-0.081	0.108	0.123	
	P	0.632	0.069	0.012	0.348	0.713	0.568	
T_cells_follicular_helper	correlation	-0.021	0.113	-0.101	0.027	-0.114	0.346	
	P	0.885	0.237	0.356	0.752	0.698	0.098	
T_cells_regulatory_Tregs	correlation	-0.036	-0.271**	-0.084	-0.022	0.021	-0.456*	
	P	0.809	0.004	0.442	0.801	0.942	0.025	
T_cells_gamma_delta	correlation	0.048	0.194*	-0.039	-0.099	-0.221	0.199	
	P	0.741	0.040	0.718	0.253	0.447	0.352	
NK_cells_resting	correlation	-0.025	0.070	0.143	0.019	-0.145	0.139	
	P	0.864	0.462	0.190	0.824	0.621	0.518	
NK_cells_activated	correlation	0.074	-0.361**	-0.255*	-0.206*	0.185	-0.170	
	P	0.612	0.000	0.018	0.016	0.527	0.427	
Monocytes	correlation	-0.088	-0.298**	-0.146	-0.053	-0.551*	-0.304	
	P	0.550	0.001	0.178	0.538	0.041	0.149	
Macrophages_M0	correlation	-0.035	0.190*	0.027	0.067	0.806**	0.030	
	P	0.810	0.045	0.808	0.436	0.000	0.889	
Macrophages_M1	correlation	0.049	0.159	0.137	-0.014	-0.142	0.011	
	P	0.738	0.093	0.209	0.868	0.627	0.961	
Macrophages_M2	correlation	0.021	0.001	0.136	0.044	-0.007	-0.290	
	P	0.888	0.995	0.211	0.615	0.980	0.169	
Dendritic_cells_resting	correlation	0.157	-0.082	-0.029	0.010	-0.181	-0.215	
	P	0.283	0.389	0.793	0.907	0.536	0.313	
Dendritic_cells_activated	correlation	-0.022	0.160	0.021	0.017	.a	0.167	
	P	0.878	0.091	0.847	0.849		0.434	
Mast_cells_resting	correlation	-0.211	-0.073	0.027	-0.220*	-0.010	-0.121	
	P	0.146	0.445	0.805	0.010	0.973	0.574	
Mast_cells_activated	correlation	0.264	0.183	-0.039	0.091	0.081	0.509*	
	P	0.066	0.054	0.718	0.293	0.782	0.011	

Contd...

Table 2: Contd...

		ID:	Hwt	IDI	Hmu	Oligo		
		TCGA	TCGA CGGA		CGGA	TCGA	CGGA	
		n=49	<i>n</i> =112	n=86	n=136	n=14	n=24	
Eosinophils	correlation	-0.085	0.262**	0.083	0.168	-0.108	0.326	
	P	0.560	0.005	0.446	0.050	0.714	0.120	
Neutrophils	correlation	0.489**	0.072	0.162	0.415**	-0.039	0.349	
	P	0.000	0.453	0.135	0.000	0.893	0.095	

TCGA = The Cancer Genome Atlas; CGGA = Chinese Glioma Genome Atlas; IDHwt = Isocitrate dehydrogenase wildtype; IDHmu = Isocitrate dehydrogenase mutant, SLC4A7: Solute Carrier Family 4 Member 7

Glioma-associated macrophages have been confirmed to originate from monocytes, supporting this phenomenon.²⁰ Moreover, the bicarbonate transporter SLC4A7 has been observed to have a notable increase in expression during macrophage differentiation, and it is essential for phagosome acidification, which strengthens the immune response.²¹ In tumor components, SLC4A7 was associated with increased proliferative stem cell populations in IDH mutant astrocytoma and oligodendroglioma, potentially driven by PIK3CA. Conversely, increased SLC4A7 was more relevant to differentiated tumor components in IDH wildtype groups. The increased SLC4A7 link to fibroblasts in all subgroups might be due to increased vessel proliferation containing abundant fibroblasts caused by SLC4A7 disruption-induced acidity. However, the exact molecular mechanisms by which SLC4A7 contributes to cancer development and progression are still not fully understood, and research in this area is ongoing.

CONCLUSION

This study underscores the potential role of SLC4A7 in adult gliomas, where its elevated expression is linked to tumor grade, poor prognosis, increased proliferation, and heightened inflammation. This research sheds light on the possible involvement of SLC4A7 in the acidic tumor microenvironment, which may contribute to cancer progression. Further investigation of SLC4A7 could provide valuable insights into cancer biology and aid in developing innovative therapeutic targets to address the unmet medical need for improved brain tumor treatments.

Author contributions

Manuscript writing: T.-L., N.-T. L., Y.-F. L.; experiment design: Y.-F. L., Y.-C. H., W.-W. H., Y.-C. L.; bioinformatics and data analysis: Y.-F. L., Y.-C. L.; conducting experiments: Y.-F. L., Y.-C. L.; reagents/materials/tools: Y.-F. L. All authors approved the final version.

Acknowledgments

English proofreading by Dr. J. C Pickles, UCL Great Ormond Street Institute of Child Health, London, UK. 210

Declarations

Ethical approval was obtained from Tri-Service General Hospital Ethics Committee (TSGHIRB No.: B-111-20).

Data availability statement

The data that support the findings of this study are available from the corresponding author, YF Li, upon reasonable request.

Financial support and sponsorship

The study funded by TSGH grants (TSGH-E-110269, TSGH-E-111269 to T. Liu; TSGH-E-110267, TSGH-D-111167 to L. nien-Tzu) and MND-MAB grant (MND-MAB-D-111109 to Y.-F. Li).

Conflicts of interest

There are no conflicts of interest.

REFERENCES

- 1. Ostrom QT, Patil N, Cioffi G, Waite K, Kruchko C, Barnholtz-Sloan JS. Corrigendum to: CBTRUS statistical report: Primary brain and other central nervous system tumors diagnosed in the united states in 2013-2017. Neuro Oncol 2022;24:1214.
- 2. Parsons DW, Jones S, Zhang X, Lin JC, Leary RJ, Angenendt P, *et al.* An integrated genomic analysis of human glioblastoma multiforme. Science 2008;321:1807-12.
- 3. Louis DN, Perry A, Wesseling P, Brat DJ, Cree IA, Figarella-Branger D, *et al.* The 2021 WHO classification of tumors of the central nervous system: A summary. Neuro Oncol 2021;23:1231-51.
- Brat DJ, Aldape K, Colman H, Figrarella-Branger D, Fuller GN, Giannini C, et al. cIMPACT-NOW update
 Recommended grading criteria and terminologies for IDH-mutant astrocytomas. Acta Neuropathol 2020;139:603-8.
- 5. Brat DJ, Aldape K, Colman H, Holland EC, Louis DN, Jenkins RB, *et al.* cIMPACT-NOW update 3: Recommended diagnostic criteria for "Diffuse astrocytic glioma, IDH-wildtype, with molecular features of

- glioblastoma, WHO grade IV". Acta Neuropathol 2018;136:805-10.
- Stupp R, Mason WP, van den Bent MJ, Weller M, Fisher B, Taphoorn MJ, et al. Radiotherapy plus concomitant and adjuvant temozolomide for glioblastoma. N Engl J Med 2005;352:987-96.
- Stupp R, Hegi ME, Mason WP, van den Bent MJ, Taphoorn MJ, Janzer RC, et al. Effects of radiotherapy with concomitant and adjuvant temozolomide versus radiotherapy alone on survival in glioblastoma in a randomised phase III study: 5-year analysis of the EORTC-NCIC trial. Lancet Oncol 2009;10:459-66.
- 8. Romero MF, Chen AP, Parker MD, Boron WF. The SLC4 family of bicarbonate (HCO₃⁻) transporters. Mol Aspects Med 2013;34:159-82.
- Millar ID, Brown PD. NBCe2 exhibits a 3 HCO3(-):1 Na+ stoichiometry in mouse choroid plexus epithelial cells. Biochem Biophys Res Commun 2008;373:550-4.
- Chen Y, Choong LY, Lin Q, Philp R, Wong CH, Ang BK, et al. Differential expression of novel tyrosine kinase substrates during breast cancer development. Mol Cell Proteomics 2007;6:2072-87.
- 11. Giannaki M, Ruf DE, Pfeifer E, Everaerts K, Heiland DH, Schnell O, *et al.* Cell-Type Dependent regulation of the electrogenic Na(+)/HCO (3)(-) cotransporter 1 (NBCe1) by hypoxia and acidosis in glioblastoma. Int J Mol Sci 2022;23:8975.
- 12. Bonneville R, Krook MA, Kautto EA, Miya J, Wing MR, Chen HZ, *et al.* Landscape of microsatellite instability across 39 cancer types. JCO Precis Oncol 2017;2017:PO.17.00073.
- 13. Le T, Phan T, Pham M, Tran D, Lam L, Nguyen T, *et al.* Browser: Making single-cell data easily accessible. bioRxiv: 2020. DOI: 10.1101/2020.12.11.414136.
- 14. Varn FS, Johnson KC, Martinek J, Huse JT,

- Nasrallah MP, Wesseling P, *et al.* Glioma progression is shaped by genetic evolution and microenvironment interactions. Cell 2022;185:2184-99.e16.
- Chen B, Khodadoust MS, Liu CL, Newman AM, Alizadeh AA. Profiling tumor infiltrating immune cells with CIBERSORT. Methods Mol Biol 2018;1711:243-59.
- Li YF, Scerif F, Picker SR, Stone TJ, Pickles JC, Moulding DA, et al. Identifying cellular signalling molecules in developmental disorders of the brain: Evidence from focal cortical dysplasia and tuberous sclerosis. Neuropathol Appl Neurobiol 2021;47:781-95.
- 17. Chang PC, Lin YC, Yen HJ, Hueng DY, Huang SM, Li YF. Ancient ubiquitous protein 1 (AUP1) is a prognostic biomarker connected with TP53 mutation and the inflamed microenvironments in glioma. Cancer Cell Int 2023;23:62.
- 18. Gorbatenko A, Olesen CW, Boedtkjer E, Pedersen SF. Regulation and roles of bicarbonate transporters in cancer. Front Physiol 2014;5:130.
- Lin HH, Tsai WC, Tsai CK, Chen SH, Huang LC, Hueng DY, et al. Overexpression of cell-surface marker SLC16A1 shortened survival in human high-grade gliomas. J Mol Neurosci 2021;71:1614-21.
- Pombo Antunes AR, Scheyltjens I, Lodi F, Messiaen J, Antoranz A, Duerinck J, et al. Single-cell profiling of myeloid cells in glioblastoma across species and disease stage reveals macrophage competition and specialization. Nat Neurosci 2021;24:595-610.
- 21. Sedlyarov V, Eichner R, Girardi E, Essletzbichler P, Goldmann U, Nunes-Hasler P, *et al.* The bicarbonate transporter SLC4A7 plays a key role in macrophage phagosome acidification. Cell Host Microbe 2018;23:766-74.e5.

Case	IDH1	TP53	KI67	SCL4A7 score	Gender	Age	Histology*	Grade	Case_41	0	0	2.02	63.74	F	65	3	2
Case 01	0	0	0.00	1.26	M	44	0	0	Case_42	0	0	0.01	1.86	F	58	3	2
Case 02	0	0	0.00	25.70	M	59	3	1	Case_43	0	0	0.19	8.44	F	30	3	2
Case 03	1	0	0.03	29.36	F	57	3	1	Case_44	0	0	0.79	57.65	F	40	3	2
Case 04	1	0	0.14	7.16	M	31	3	1	Case_45	0	0	0.06	21.53	F	16	3	2
Case_05	1	0	0.01	6.14	M	30	3	1	Case_46	1	0	0.58	41.33	F	47	3	2
Case 06	0	0	0.31	17.52	M	49	3	1	Case_47	0	0	0.77	51.84	F	32	3	2
Case_07	1	0	0.03	26.93	M	52	3	2	Case_48	0	0	1.89	75.11	M	63	3	2
Case_08	1	0	0.48	15.03	F	50	3	1	Case_49	0	0	0.01	28.31	F	18	3	2
Case 09	1	0	0.02	22.87	M	49	3	1	Case_50	0	0	1.59	36.10	M	43	3	2
Case_10	1	0	0.69	9.18	M	47	3	2	Case_51	0	0	0.95	43.46	F	50	3	3
Case_11	0	0	0.07	37.23	F	19	3	2	Case_52	1	1	1.19	16.59	F	32	3	3
Case 12	1	1	0.42	19.38	F	40	3	2	Case_53	0	1	2.87	10.19	M	43	3	3
Case_13	1	1	0.98	13.98	M	36	3	2	Case_54	1	1	0.51	25.45	M	35	3	3
Case_14	1	0	0.02	2.04	M	56	3	2	Case_55	0	0	0.01	2.04	М	65	3	4
Case_15	0	0	0.00	4.90	M	40	3	2	Case_56	0	0	0.02	7.97	F	58	3	2
Case_16	1	1	1.41	36.35	M	56	3	2	Case_57	0	1	0.33	2.80	M	66	3	4
Case_17	1	1	1.03	28.42	M	53	3	2	Case_58	1	0	4.90	31.98	M F	71	1	3
Case 18	0	0	1.55	6.23	M	32	3	2	Case_59	0	0	3.54	46.88		61	3	3
Case_19	1	0	0.01	15.75	M	48	3	2	Case_60	0	1	6.00 0.03	24.05	F	6	3	4
Case_20	0	0	0.04	16.60	F	40	3	2	Case_61		0		5.77	M	59	3	4
Case_21	0	0	0.08	16.04	F	40	3	2	Case_62	0	0	1.22 0.12	37.47 25.25	M M	9 64	3	4
Case_22	1	0	0.72	11.52	M	47	3	2	Case_63	0	1	14.73			23		3
Case_23	0	0	0.87	2.27	F	45	3	2	Case_64	0	0	0.75	85.78 0.76	M F	23 67	3	
Case_24	1	0	0.91	33.31	M	46	1	2	Case_65	0	0	0.73	1.75	F	58	2	4
Case_25	1	0	0.54	8.28	M	32	3	2	Case_66	0	0	23.57	19.89	F	50	3	4
Case_26	0	0	0.28	0.35	F	26	3	2	Case_67 Case_68	1	0	0.53	35.47	F	40	3	4
Case_27	0	0	0.00	1.37	F	30	3	2	Case 69	0	0	4.25	22.49	F	59	3	2
Case_28	1	0	1.25	28.19	F	49	3	2	Case_70	1	0	1.15	69.00	M	55	1	3
Case_29	0	0	0.52	32.53	M	45	3	2	Case_70	1	0	0.20	19.49	M	66	2	3
Case_30	0	0	0.02	19.15	M	53	3	2	Case_71	1	0	0.08	18.98	M	29	1	2
Case_31	1	0	0.02	15.97	F	41	3	2	Case_72	0	0	3.13	44.90	M	54	1	2
Case_32	0	0	3.80	20.47	M	57	3	2	Case_74	0	0	0.02	4.65	F	55	2	2
Case_33	0	0	0.08	12.96	M	50	3	2	Case_75	0	0	0.00	2.81	F	38	0	0
Case_34	0	0	0.83	16.67	F	48	3	2	Case_76	0	0	0.00	4.57	F	42	0	0
Case_35	0	0	7.00	30.77	F	41	3	2	Case_77	0	0	0.00	12.82	M	35	0	0
Case_36	1	0	0.02	21.07	M	48	3	2	Case_78	0	0	0.00	13.89	M	26	0	0
Case_37	0	0	1.05	51.14	M	34	3	2	Case_79	0	0	0.01	19.44	M	45	0	0
Case_38	0	1	2.07	43.26	M	44	3	2	Case_80	0	0	0.00	0.87	M	49	0	0
Case_39	1	1	3.30	74.68	F	28	3	2	Case_81	0	0	0.01	11.36	M	48	0	0
Case_40	0	0	22.40	31.34	M	45	3	3	Case_82	0	0	0.02	3.12	F	21	0	0
								ontd	*0: normal								

Contd... *0

*0: normal; 1: oligodendroglioma; 2:oligoastrocytoma; 3: astrocytoma